



Article

Computational Dynamics of Multi-Rigid-Body System in Screw Coordinate

Jing-Shan Zhao * , Song-Tao Wei  and Xiao-Cheng Sun

State Key Laboratory of Tribology, Department of Mechanical Engineering, Tsinghua University, Beijing 100084, China; wei-st18@mails.tsinghua.edu.cn (S.-T.W.); sxs21@mails.tsinghua.edu.cn (X.-C.S.)
* Correspondence: jingshanzhao@mail.tsinghua.edu.cn; Fax: +86-10-6278-7173

Abstract: This paper investigates the kinematics and dynamics of multi-rigid-body systems in screw form. The Newton–Euler dynamics equations are established in screw coordinates. All forces and torques of the multi-rigid-body system can be solved straightforwardly since they are explicit in the form of screw coordinates. The displacement and acceleration are unified in matrix form, which associates the kinematics and dynamics with variable of velocity. A one-step numerical algorithm only is needed to solve the displacements and accelerations. As a result, all absolute displacements, velocities, and accelerations are directly obtained by one kinematic equation. The kinematics and dynamics of Gough–Stewart platform validate this the method. In this paper, the kinematics and dynamics are carried out with the example of a Gough–Stewart platform, which represents the most complex multi-rigid-body system, to verify the computational dynamics method. The proposed algorithm is also fit for the kinematics and dynamics modeling of other multi-rigid-body systems.

Keywords: multi-rigid-body system; screw coordinate; kinematics; dynamics



Citation: Zhao, J.-S.; Wei, S.-T.; Sun, X.-C. Computational Dynamics of Multi-Rigid-Body System in Screw Coordinate. *Appl. Sci.* **2023**, *13*, 6341. <https://doi.org/10.3390/app13106341>

Academic Editor: Alessandro Gasparetto

Received: 3 April 2023
Revised: 11 May 2023
Accepted: 18 May 2023
Published: 22 May 2023



Copyright: © 2023 by the authors. Licensee MDPI, Basel, Switzerland. This article is an open access article distributed under the terms and conditions of the Creative Commons Attribution (CC BY) license (<https://creativecommons.org/licenses/by/4.0/>).

1. Introduction

It is well known that a multi-rigid-body system is normally a complex system with many links and joints and is fundamental for mechanism research in robotics, spacecraft, and bionic areas. Studies of multi-rigid-body systems can neglect the flexibility of the bodies and focus on the kinematic and dynamic performance of the mechanisms. Extensive research has proposed a series of theoretical models of multi-rigid-body systems. Parallel mechanisms are common multi-rigid-body systems with high loading ability, good dynamic response, and precise motion. The Gough–Stewart platform as a common parallel mechanism is proposed as a flight simulator by Gough and Stewart [1–3], which has high flexibility. Therefore, the study of the kinematics and dynamics of the Gough–Stewart platform is vital research topics for its application.

Dynamics analysis has theoretical and practical significance for realizing robot control, stability in motion, and optimization in structure. Scholars presented some dynamics methods for parallel mechanisms. The widely-used methods for multi-rigid-body system dynamics mainly include Lagrange equation [4,5], Newton–Euler equation [6], virtual work principle equation [7,8], Kane equation [9], and Gibbs–Appell equation [10]. The Newton–Euler dynamics equation for the Gough–Stewart platform, which is based on the vector method and proposed by Dasgupta, is a classic algorithm in dynamics modeling [11,12]. Newton–Euler equations can express the rotational and translational motion of a rigid body in the absolute coordinate system. Through a single equation with six components in the form of column vectors and matrix, the forces and moments acting on the rigid body and the motion of the center of mass of a rigid body can be combined [13–15]. Gallardo-Alvarado [16,17] proposed dynamics analysis of parallel mechanisms by screw coordinates and the principle of virtual work. The analysis of a multi-rigid-body system is usually solved through analytical methods in classical mechanics and vector equations [18–21].

The displacement, velocity, and acceleration obtained in kinematics are essential information for dynamics modeling. To describe the kinematics of a mechanism, the translational and rotational motions should be expressed with a suitable mathematical framework in a relatively general way [22,23]. Meanwhile, there are also several finite solutions corresponding to different configurations of a multi-rigid-body system [24–26]. The kinematics modeling of a multi-rigid-body system can be simplified by resorting to screw coordinates. Many researchers have utilized screw coordinates in kinematics analysis [27,28] of parallel mechanisms.

This paper focuses on the kinematics and dynamics of a multi-rigid-body system by the Newton–Euler method in screw coordinate. From kinematics analysis, the absolute displacement, velocity, and acceleration of each joint and link can be derived in the absolute coordinate frame, which can be applied directly in dynamics. This method would be much clearer and more straightforward not only for the inverse dynamics problem but also for the derivation of closed-form dynamics formulae.

2. Kinematics of a Multi-Rigid-Body System

This section presents the method for establishing the kinematics of a multi-rigid-body system based on screw coordinates. Velocity screw is defined to unify the angular velocity and linear velocity of a joint. With the velocity screw equation, the relative velocity of each joint can be obtained. Then, both displacement and acceleration are calculated by a one-step numerical method. Based on the linear superposition principle, the absolute displacement, velocity, and acceleration of each joint can be derived uniformly in screw coordinates.

2.1. Relative Displacement, Velocity and Acceleration of Each Joint

In Figure 1a, for a multi-rigid-body system, there are p kinematic chains each of which has n joints. In the multi-rigid-body system, L represents a link, j represents a joint and $loop$ represents a kinematic chain. As shown in Figure 1b, suppose L_{i-1} and L_{i-2} are two rigid bodies in a serial kinematic chain which are connected by joint j_{i-1} .

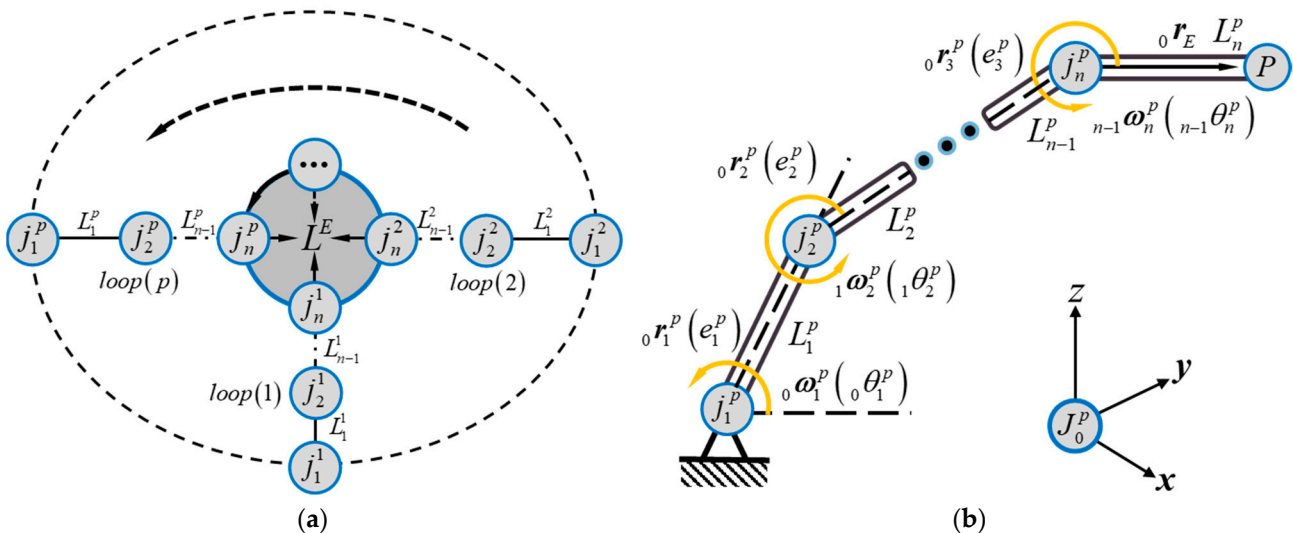


Figure 1. A multi-rigid-body system: (a) multi-rigid-body system; (b) a serial kinematic chain.

The dual 3-dimensional vectors, ${}^0\omega_1^p$ and ${}^0v_1^p$, can fully determine the motion of link L_1^p . Its velocity screw vector can be defined as

$${}^0V_1^p = \begin{bmatrix} {}^0\omega_1^p \\ {}^0v_1^p \end{bmatrix} \tag{1}$$

where ${}_0\omega_1^p$ is the relative angular velocity vector of joint j_1^p with respect to the grounded link 0, ${}_0v_1^p$ is the relative linear velocity of a point on the link L_1^p with its extended body that is passing through the origin of the absolute coordinate frame at this instant.

The 3-dimensional vector ${}_0v_1^p$ can be expressed by ${}_0v_1^p = {}_0r_1^p \times {}_0\omega_1^p$ where ${}_0r_1^p$ is the position vector of joint j_1^p with respect to the origin of the grounded coordinate frame.

Suppose $\|e_1^p\| = 1$, Equation (1) can be rewritten as

$${}_0V_1^p = {}_0\omega_1^p \begin{bmatrix} e_1^p \\ {}_0r_1^p \times e_1^p \end{bmatrix} \tag{2}$$

where e_1^p is the direction vector of joint j_1^p in the absolute coordinate frame, and ${}_0\omega_1^p$ is the relative angular speed of joint j_1^p in the absolute coordinate frame. Let

$$S_1^p = \begin{bmatrix} e_1^p \\ {}_0r_1^p \times e_1^p \end{bmatrix} \tag{3}$$

where S_1^p is the unit screw of joint j_1^p .

Substituting Equation (3) into Equation (2) yields

$${}_0V_1^p = {}_0\omega_1^p S_1^p \tag{4}$$

For a kinematic chain $loop(p)$ shown in Figure 1a, based on the linear combination, the kinematics of the end joint j_1^p can be expressed as:

$$\begin{cases} {}_0\omega_n^p = {}_0\omega_1^p + {}_1\omega_2^p + {}_2\omega_3^p + \dots + {}_{n-2}\omega_{n-1}^p + {}_{n-1}\omega_n^p \\ {}_0v_n^p = {}_0v_1^p + {}_1v_2^p + {}_2v_3^p + \dots + {}_{n-2}v_{n-1}^p + {}_{n-1}v_n^p \end{cases} \tag{5}$$

In accordance with Equation (2), the forward kinematics of a single kinematic chain can be rewritten as:

$${}_0V_n^p = \sum_{i=0}^n {}_iV_{i+1}^p = S^p \omega^p \tag{6}$$

where

$$S^p = [S_1^p \ S_2^p \ \dots \ S_n^p] \tag{7}$$

which represents the unit screw matrix of the single kinematic chain $loop(p)$ and

$$\omega^p = [{}_0\omega_1^p \ {}_1\omega_2^p \ \dots \ {}_{n-1}\omega_n^p]^T \tag{8}$$

where ${}_{n-1}\omega_n^p$ is the relative angular speed of the link L_n^p with respect to the link L_{n-1}^p connecting joint j_{n-1}^p .

With the definition of the twist matrix and Equation (6), the velocity screw equation of a multi-rigid-body system would be obtained,

$$S\omega = V \tag{9}$$

where

$$S = \text{diag}[S^1 \ S^2 \ \dots \ S^p]_{6p \times 6p} \tag{10}$$

in which S^p is the unit screw matrix of the single kinematic chain $loop(p)$, and $\text{diag}[\]$ is a diagonal matrix of S^1, S^2, \dots, S^p .

And

$$\omega = [(\omega^1)^T \ (\omega^2)^T \ \dots \ (\omega^p)^T]^T_{6p \times 1} \tag{11}$$

in which ω^p is the vector of relative angular speeds of all joints in the single kinematic chain $loop(p)$, and

$$V = \left[\begin{matrix} ({}_0V_n^1)^T & ({}_0V_n^2)^T & \cdots & ({}_0V_n^p)^T \end{matrix} \right]_{6p \times 1}^T \tag{12}$$

in which ${}_0V_n^p$ is the vector of the absolute velocity screw of the n th joint in the single kinematic chain $loop(p)$. Equation (10) is the screw matrix of the multi-rigid-body system. Equation (11) is a velocity vector composed of the relative angular speeds of each generalized joint with respect to its previous link. Equation (12) is the velocity vector of each end joint in the absolute coordinate frame.

With Equation (6), when the kinematics of the terminal link j_n is specified, its inverse kinematics of the multi-rigid-body system can be derived,

$$S^T S \omega = S^T V \tag{13}$$

When $|S^T S| = 0$, the multi-rigid-body system is either redundantly actuated or in singularity configuration. Otherwise, we gain the angular speeds of all joints from Equation (13):

$$\omega = [S^T S]^{-1} S^T V \tag{14}$$

where $[S^T S]^{-1} S^T$ is called the pseudo inverse of screw matrix S . Equation (14) represents the inverse velocity of the multi-rigid-body system. Based on Equation (14), we get the steps to calculate the inverse kinematics of a multi-rigid-body system below:

1. With the initial condition consisting of position angles ${}_{n-1}\theta_n^p(t = 0)$ and structure parameters R, r , and l_n^p , the unit screw matrix $S(0)$ of the multi-rigid-body system at time $t = 0$ can be gained first.
2. Substituting $S(0)$ into Equation (14) and with the twist matrix $\$n^p$ of the end joint j_n^p in Equation (7) being known, the relative angular velocity of each joint $\omega(0)$ at time $t = 0$ can be derived.
3. With the initial conditions consisting of position and velocity, the parameters of $\$n^p(k)$ from Equation (10) and $\omega(k)$ from Equation (14) could be updated by steps 1 and 2 where $t = 0$ is replaced by $t = k\Delta t$:

$${}_{n-1}\theta_n^p((k+1)\Delta t) = {}_{n-1}\theta_n^p(k\Delta t) + \Delta t \omega(k) \tag{15}$$

where $k = 1, 2, \dots$.

With the unit screw matrix $S(k)$, the position vector, ${}_0r_n^p$, and orientation vector, e_n^p , of each joint can be deduced from Equation (14).

2.2. Absolute Displacement, Velocity, and Acceleration of Each Joint

Due to the linear superposition principle, the absolute velocity of the n th joint at the absolute coordinate frame is expressed by

$${}_0V_n(k+1) = \sum_{i=1}^n {}_iV_i(k+1) \tag{16}$$

Suppose ${}_0D_n = \begin{bmatrix} {}_0\theta_n^p \\ {}_0d_n^p \end{bmatrix}$, in which ${}_0D_n$ is the absolute displacement vector of each joint that consists of absolute angular displacement ${}_0\theta_n$ and absolute linear displacement ${}_0d_n$. Suppose ${}_0A_n = \begin{bmatrix} {}_0\beta_n \\ {}_0a_n \end{bmatrix}$, in which ${}_0A_n$ is the absolute acceleration vector of each joint that consists of absolute angular acceleration ${}_0\beta_n$ and absolute linear acceleration ${}_0a_n$.

The absolute displacement and acceleration of each joint at the absolute coordinate frame can be expressed by the simplest one-step numerical algorithm,

$$\begin{cases} {}_0D_n(k+1) = {}_0D_n(k) + \Delta t {}_0V_n(k) \\ {}_0A_n(k+1) = \frac{{}_0V_n(k+1) - {}_0V_n(k)}{\Delta t} \end{cases} \quad (17)$$

The absolute velocity screw matrix ${}_0V_n$, the absolute displacement vector ${}_0D_n$, and the absolute acceleration vector ${}_0A_n$ can be obtained by calculating the angular displacement ${}_{n-1}\theta_n^p(t=0)$ with Equation (15). The results can be applied to the kinematics analysis of any point on a single-rigid-body.

2.3. Absolute Displacement, Velocity and Acceleration of Each Rigid-Body

Suppose there is a point P on the rigid-body L_n^p , and the velocity of the point P on the rigid-body L_n^p is hence represented as

$${}_0v_n^P = {}_0v_n + {}_0\omega_n \times {}_0r_P \quad (18)$$

where ${}_0r_P$ indicates the position vector of the point P in the absolute ground coordinate frame 0.

For a kinematic chain $loop(p)$ shown in Figure 1b, the absolute angular and linear velocities of the point P on the rigid-body L_n^p can be expressed as:

$$\begin{cases} {}_0\omega_n^P = {}_0\omega_1^p + {}_1\omega_2^p + {}_2\omega_3^p + \dots + {}_{n-2}\omega_{n-1}^p + {}_{n-1}\omega_n^p \\ {}_0v_n^P = {}_0v_1^p + {}_1v_2^p + {}_2v_3^p + \dots + {}_{n-2}v_{n-1}^p + {}_{n-1}v_n^p + {}_0\omega_n^P \times {}_0r_P \end{cases} \quad (19)$$

Consequently, the velocity of a point P on the rigid-body L_n^p is expressed in the screw coordinates below

$${}_0V_n^P = {}_0V_n + \begin{bmatrix} 0 \\ {}_0\omega_n^P \times {}_0r_P \end{bmatrix} \quad (20)$$

The absolute acceleration vector of point P on the rigid-body L_n^p can be derived in a similar one-step numerical algorithm in Equation (17):

$$\begin{cases} {}_0D_n^P(k+1) = \sum_{i=1}^n {}_{n-1}D_n^P(k) + \Delta t {}_{n-1}V_n^P(k) \\ {}_0A_n^P(k+1) = \sum_{i=1}^n \frac{{}_{n-1}V_n^P(k+1) - {}_{n-1}V_n^P(k)}{\Delta t} \end{cases} \quad (21)$$

The absolute acceleration of a point on the rigid-body in the absolute ground coordinate frame 0 can be directly used in the Newton-Euler dynamics of a multi-rigid-body system. The procedures of the above calculation are illustrated in Figure 2.

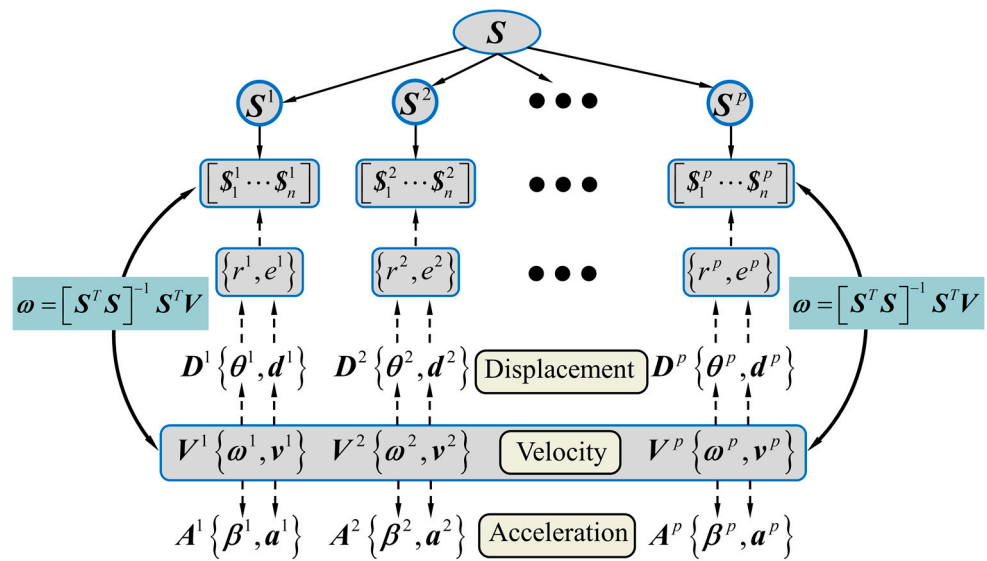


Figure 2. The procedure for the kinematics on multi-rigid-body system.

3. Dynamics of a Multi-Rigid-Body System

The dynamics of a rigid body was described by the Newton–Euler equations in classical mechanics. Euler’s two laws of motion for a rigid body are grouped together into a single equation by the Newton–Euler equation. When the external loads, constraint forces, and self-weights of all bodies are taken into account in the calculation of wrenches, the balance conditions for a single-rigid-body will be

$$\begin{bmatrix} T \\ F \end{bmatrix} = \begin{bmatrix} J_n & 0 \\ 0 & m_n I \end{bmatrix} \begin{bmatrix} \beta \\ a \end{bmatrix} + \begin{bmatrix} \omega \times J_n \omega \\ m_n g \end{bmatrix} \tag{22}$$

where $T = T^n - T^{n-1}$ is the resultant torque of a single-rigid-body, in which T^n is the constraint torque vector at joint j_n , $F = F^n - F^{n-1}$ is the resultant force of a single-rigid-body, in which F^n is the constraint force vector at joint j_n , I is an identity matrix of 3×3 , m_n is the mass of a single-rigid-body, a is the absolute linear acceleration at the mass center, β is the absolute angular acceleration, and ω is the absolute angular velocity. Figure 3 demonstrates the Newton-Euler parameters of two adjacent bodies in a multi-rigid-body system.

$$J_0 = R_{0n} J_n R_{0n}^T \tag{23}$$

where J_0 is the matrix of mass moment of inertia of a single-rigid-body at its mass center in the absolute coordinate frame (coordinate frame 0), J_n is the matrix of mass moment of inertia of a single-rigid-body at its principal coordinate frame of the mass center (coordinate frame n), and R_{0n} is the rotation matrix from the coordinate frame n to the coordinate frame 0.

The Newton–Euler equations of dynamics of the multi-rigid-body system can be therefore be written as:

$$CW^S = MA^M + W^C + W^E \tag{24}$$

where $W^S = \begin{bmatrix} [T_1]^T \\ [F_1]^T \end{bmatrix} \begin{bmatrix} [T_2]^T \\ [F_2]^T \end{bmatrix} \dots \begin{bmatrix} [T_n]^T \\ [F_n]^T \end{bmatrix} \begin{bmatrix} [T_n]^T \\ [F_n]^T \end{bmatrix}^T$ is the constraint wrench matrix of a multi-

rigid-body system including all constraint forces and constraint torques, W^C is the Coriolis wrench matrix of the multi-rigid-body system, W^E is the external wrench matrix exerted at the multi-rigid-body system which also includes the gravity, C is the displacement matrix, M is the mass matrix, and A^M is the acceleration matrix composed by the absolute accelerations of the mass centers in the multi-rigid-body system.

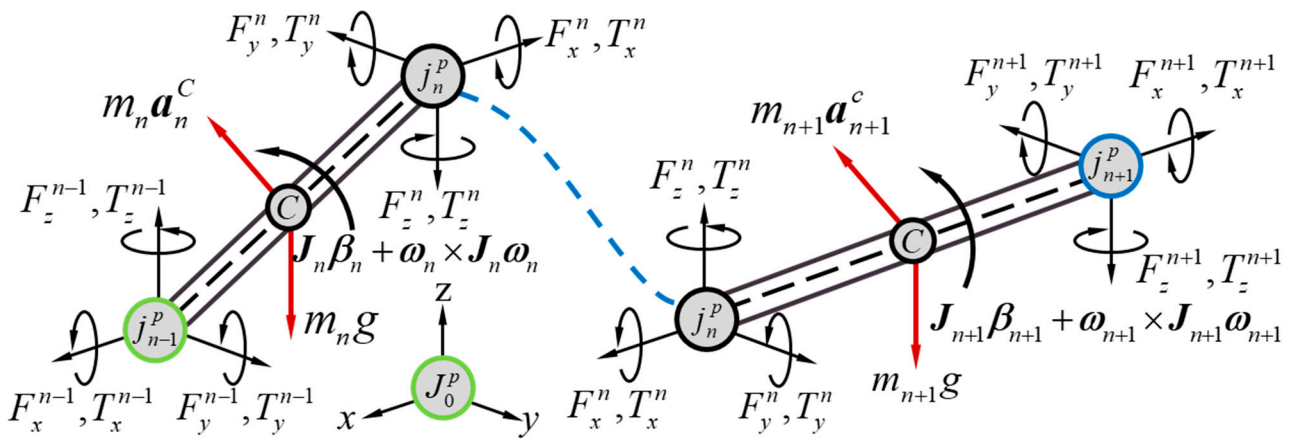


Figure 3. Newton-Euler parameters.

When the number of constraint wrenches equals the number of equations in Equation (24), the supporting wrench can be calculated by

$$W^S = (CC^T)^{-1} (MA^M + W^C + W^E) \tag{25}$$

4. Kinematics and Dynamics of the Gough–Stewart Platform

In this section, an application of the above method will be presented in the example of the Gough–Stewart platform. As shown in Figure 4, the Gough–Stewart platform consists of six kinematic chains, which are composed of a spherical joint, a prismatic joint and a universal joint. To simplify the expression of the kinematic chains, the spherical joint, prismatic joint, and universal joint are presented by the capital of the first letter of the joint name: S, P, and U, respectively. The prismatic joint P is the actuated joint in the multi-rigid-body system. The Gough–Stewart platform has a fixed base and a moving manipulator connected by six extendable legs through universal joints at both ends.

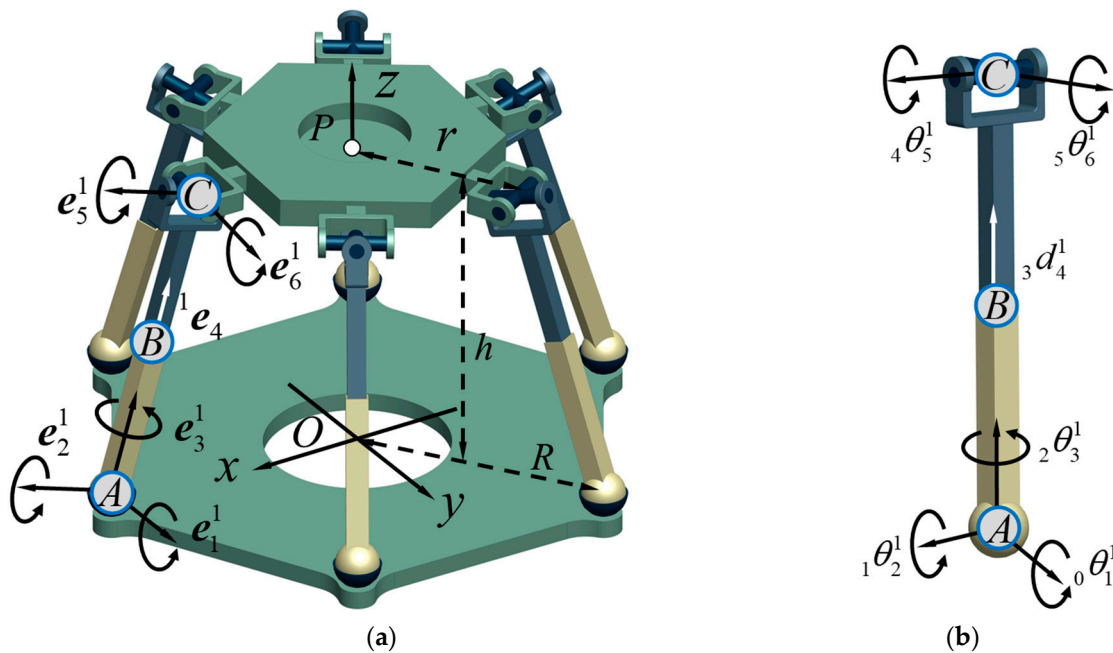


Figure 4. Kinematics analysis of the Gough–Stewart platform: (a) kinematics of the Gough–Stewart platform; (b) initial condition of the first kinematic chain.

4.1. Kinematics Analysis of the Gough–Stewart Platform

This section gives the inverse kinematics analysis of the Gough–Stewart platform. As shown in Figure 4, the inverse kinematics of the Gough–Stewart platform can be expressed as:

$$S\omega = V_C \tag{26}$$

where $S = \text{diag}[S^1 \ S^2 \ S^3 \ S^4 \ S^5 \ S^6]$ in which $S^p = [s_1^p \ s_2^p \ s_3^p \ s_4^p \ s_5^p \ s_6^p]$, and $s_1^p = \begin{bmatrix} e_1^p \\ {}_0r_A^p \times e_1^p \end{bmatrix}$, $s_2^p = \begin{bmatrix} e_2^p \\ {}_0r_A^p \times e_2^p \end{bmatrix}$, $s_3^p = \begin{bmatrix} e_3^p \\ {}_0r_A^p \times e_3^p \end{bmatrix}$, $s_4^p = \begin{bmatrix} 0 \\ e_4^p \end{bmatrix}$, $s_5^p = \begin{bmatrix} e_5^p \\ {}_0r_C^p \times e_5^p \end{bmatrix}$, $s_6^p = \begin{bmatrix} e_6^p \\ {}_0r_C^p \times e_6^p \end{bmatrix}$, $p = 1, 2, \dots, 6$, $\omega = [\omega^1 \ \omega^2 \ \omega^3 \ \omega^4 \ \omega^5 \ \omega^6]^T$ and where $\omega^1 = [{}_{1}\omega_1^1 \ {}_{1}\omega_2^1 \ {}_{2}\omega_3^1 \ {}_{3}\omega_4^1 \ {}_{4}\omega_5^1 \ {}_{5}\omega_6^1]^T$.

To get the unit screws in Equation (26), the rotation matrix is applied to express e_n^p, r_n^p of each joint in the local coordinate frame, p represents the p th chain, and n represents the n th joint in a chain.

$$\begin{cases} e_n^p = R_Z^p \left(\prod_{n=2}^p R_n^p \right) e_n^p(0) \\ r_n^p = R_Z^p \left({}_0r_A^p(0) + R_2^p R_3^p R_5^p r_{AC}^p \right) \end{cases}, \begin{cases} (n = 1, 2, \dots, 6) \\ (p = 1, 2, \dots, 6) \end{cases} \tag{27}$$

where R_Z^p is the rotation matrix around z axis, which can be expressed as: $R_Z^p = R_z(\frac{\pi}{6}(p - 1))$. R_n^p is the rotation matrix from link L_n to link L_{n-1} , when it rotates around x-axis, $R_n^p = R_x({}_{n-1}\theta_n^p)$, when it rotates around y-axis, $R_n^p = R_y({}_{n-1}\theta_n^p)$, and when it rotates around z-axis, $R_n^p = R_z({}_{n-1}\theta_n^p)$. The initial condition parameters are illustrated in Table 1, and $I_{(3 \times 3)}$ is an identity matrix of 3×3 .

Table 1. Initial conditions and rotation matrix of Gough–Stewart platform.

| | | | | | | |
|-----------------------------------|-------------------------------|----------------------------------|----------------------------------|-------------------------------|----------------------------------|----------------------------------|
| Initial posture | $e_1^1(0)$ $[0 \ 1 \ 0]^T$ | $e_2^1(0)$ $[1 \ 0 \ 0]^T$ | $e_3^1(0)$ $[0 \ 0 \ 1]^T$ | $e_4^1(0)$ $[0 \ 0 \ 0]^T$ | $e_5^1(0)$ $[1 \ 0 \ 0]^T$ | $e_6^1(0)$ $[0 \ 1 \ 0]^T$ |
| Initial position | $r_A^1(0)$ $[R \ 0 \ 0]^T$ | $r_B^1(0)$ $[0 \ 0 \ L]^T$ | $r_C^1(0)$ $[0 \ 0 \ 2L]^T$ | | | |
| Homogeneous transformation matrix | R_1^p I | R_2^p $T_y({}_0\theta_1^p)$ | R_3^p $T_x({}_1\theta_2^p)$ | R_4^p I | R_5^p $T_z({}_2\theta_3^p)$ | R_6^p $T_x({}_4\theta_5^p)$ |

After knowing the velocity screw of the moving platform at its mass center in the absolute coordinate frame, the relative angular velocity of each chain L^p , ($p = 1, 2 \dots 6$) can be derived based on Equation (14):

$$\omega = [S^T S]^{-1} S V_C^p \tag{28}$$

where V_C^p , ($p = 1, 2 \dots 6$) is the velocity screw of joint j_C , which can be expressed as:

$$V_C^p = V_P - {}_C V_P^p \tag{29}$$

where V_P is the velocity screw of the reference point P on the moving platform, and it is given for the inverse kinematics. ${}_C V_P^p, (p = 1, 2 \dots 6)$ is the relative kinematics screw from joint $j_C^p, (p = 1, 2 \dots 6)$ to the reference point P on the moving platform. It can be expressed as:

$${}_C V_P^p = \begin{bmatrix} 0 \\ {}_0 \omega_C^p \times {}_0 r_P^p \end{bmatrix} \tag{30}$$

where ${}_0 \omega_C^p, (p = 1, 2 \dots 6)$ is the absolute angular velocity of the moving platform, and ${}_0 r_P^p, (p = 1, 2 \dots 6)$ is the absolute position vector of the reference point P on the moving platform.

4.2. Dynamics Analysis of the Gough–Stewart Platform

a. Inverse dynamics equations for the fixed leg $L_{AB}^p, (p = 1, 2 \dots 6)$

The fixed leg $L_{AB}^p, (p = 1, 2 \dots 6)$ consists of one spherical joint and one prismatic joint, which is shown in Figure 5b. At spherical joint $j_A^p, (p = 1, 2 \dots 6)$, there are three forces F_A without torque. At prismatic joint $j_B^p, (p = 1, 2 \dots 6)$, there are three forces F_B and three torques T_B . The dynamics equations for the fixed leg $L_{AB}^p, (p = 1, 2 \dots 6)$ can be derived:

$$\begin{bmatrix} {}_A r_D \times F_A - {}_D r_B \times F_B - T_B \\ F_A - F_B \end{bmatrix} = \begin{bmatrix} J_D & 0 \\ 0 & m_D I \end{bmatrix} \begin{bmatrix} \beta_D \\ a_D \end{bmatrix} + \begin{bmatrix} \omega_D \times J_D \omega_D \\ m_D g \end{bmatrix} \tag{31}$$

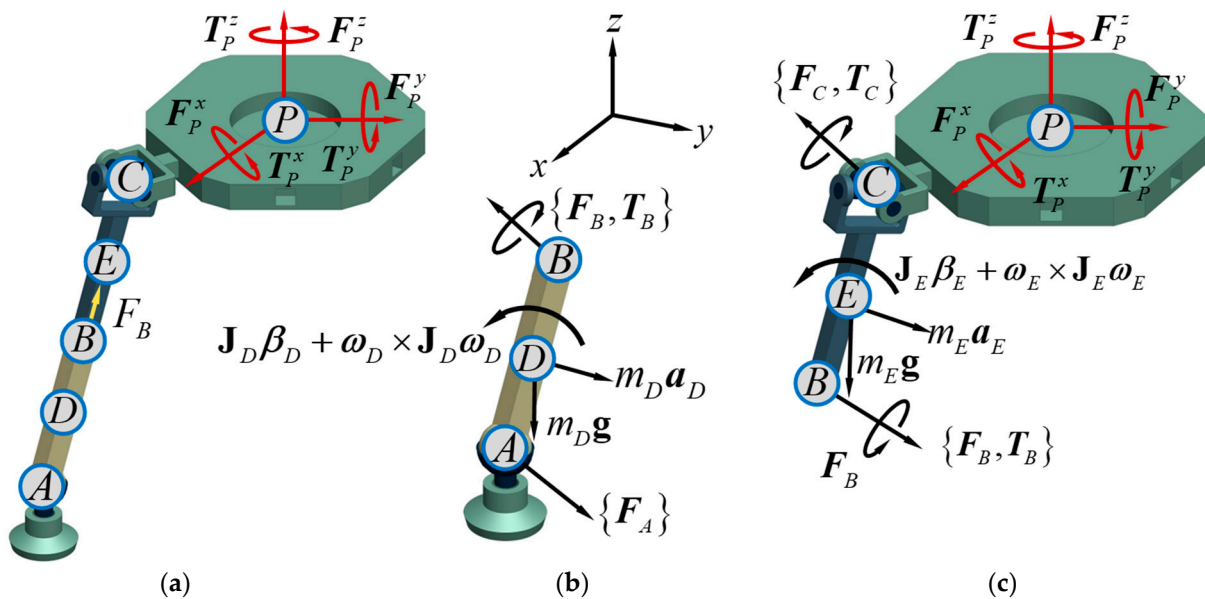


Figure 5. Dynamic analysis of the Gough–Stewart platform: (a) dynamics of the first kinematic chain; (b) dynamics of the fixed leg $L_{AB}^p, (p = 1, 2 \dots 6)$; (c) dynamics of the moving leg $L_{BC}^p, (p = 1, 2 \dots 6)$.

b. Inverse dynamics equations for the moving leg $L_{BC}^p, (p = 1, 2 \dots 6)$

The moving leg $L_{BC}^p, (p = 1, 2 \dots 6)$ consists of one universal joint and one prismatic joint which is shown in Figure 5c. At universal joint $j_C^p, (p = 1, 2 \dots 6)$, there are three forces F_C and one torque T_C , the direction of the torque T_C at joint $j_C^p, (p = 1, 2 \dots 6)$ is along the leg. At prismatic joint $j_B^p, (p = 1, 2 \dots 6)$, there are three forces F_B and three torques T_B . The dynamics equations for the fixed leg $L_{BC}^p, (p = 1, 2 \dots 6)$ can be expressed by

$$\begin{bmatrix} {}_B r_E \times F_B - {}_E r_C \times F_C + T_B - T_C \\ F_B - F_C \end{bmatrix} = \begin{bmatrix} J_E & 0 \\ 0 & m_E I \end{bmatrix} \begin{bmatrix} \beta_E \\ a_E \end{bmatrix} + \begin{bmatrix} \omega_E \times J_E \omega_E \\ m_E g \end{bmatrix} \tag{32}$$

c. *Inverse dynamics equations for the moving platform L_P*

The moving platform L_P consists of six universal joints j_C^p , ($p = 1, 2 \dots 6$), which are shown in Figure 5c. At the universal joint j_C^p , ($p = 1, 2 \dots 6$), there are three forces F_C and one torque T_C . Suppose that there is an external force system (if any) acting on the moving platform, which consists of a force F_P and a torque T_P in the absolute coordinate frame. The dynamics equations for the moving platform L_P are expressed by

$$\begin{bmatrix} \sum_{p=1}^6 ({}^0r_C \times F_C) + \sum_{p=1}^6 T_C \\ \sum_{p=1}^6 F_C \end{bmatrix} = \begin{bmatrix} J_P & 0 \\ 0 & m_P \mathbf{I} \end{bmatrix} \begin{bmatrix} \beta_P \\ a_P \end{bmatrix} + \begin{bmatrix} \omega_P \times J_P \omega_P \\ m_P \mathbf{g} \end{bmatrix} + \begin{bmatrix} T_P \\ F_P \end{bmatrix} \quad (33)$$

d. *Inverse dynamics equations for Gough–Stewart platform*

Suppose,

$$W^S = [F_A \quad F_B \quad F_C \quad T_B \quad T_C] \quad (34)$$

where $F_A = [F_A^1 \quad F_A^2 \quad \dots \quad F_A^6]^T$, in which F_A^1 is the supporting force at joint j_A^1 , and F_A^1 can be expressed by a 3-dimensional vector, and $T_B = [T_B^1 \quad T_B^2 \quad \dots \quad T_B^6]^T$, in which T_B^1 is the supporting torque at joint j_B^1 , and T_B^1 can be expressed by a 3-dimensional vector.

Suppose,

$$C = \begin{bmatrix} {}^A\hat{r}_D & -{}^D\hat{r}_B & \mathbf{0}_{(18 \times 18)} & -\mathbf{I}_{(18 \times 18)} & \mathbf{0}_{(18 \times 6)} \\ \mathbf{I}_{(18 \times 18)} & -\mathbf{I}_{(18 \times 18)} & \mathbf{0}_{(18 \times 18)} & \mathbf{0}_{(18 \times 18)} & \mathbf{0}_{(18 \times 6)} \\ \mathbf{0}_{(18 \times 18)} & {}^B\hat{r}_E & -{}^E\hat{r}_C & \mathbf{I}_{(18 \times 18)} & -{}^Ae_{C(18 \times 6)} \\ \mathbf{0}_{(18 \times 18)} & \mathbf{I}_{(18 \times 18)} & -\mathbf{I}_{(18 \times 18)} & \mathbf{0}_{(18 \times 18)} & \mathbf{0}_{(18 \times 6)} \\ \mathbf{0}_{(3 \times 18)} & \mathbf{0}_{(3 \times 18)} & -{}^P\hat{r}_C & \mathbf{0}_{(3 \times 18)} & -{}^Ae_{C(3 \times 6)} \\ \mathbf{0}_{(3 \times 18)} & \mathbf{0}_{(3 \times 18)} & -\mathbf{I}_{(3 \times 18)} & \mathbf{0}_{(3 \times 18)} & \mathbf{0}_{(3 \times 6)} \end{bmatrix} \quad (35)$$

where $\mathbf{I}_{(n \times n)}$ is an identity matrix of $n \times n$, $\mathbf{I}_{(3 \times 18)} = [\mathbf{I}_{(3 \times 3)} \quad \mathbf{I}_{(3 \times 3)} \quad \mathbf{I}_{(3 \times 3)} \quad \mathbf{I}_{(3 \times 3)} \quad \mathbf{I}_{(3 \times 3)} \quad \mathbf{I}_{(3 \times 3)}]$, and $\mathbf{0}_{(n \times m)}$ is a zero-matrix. In Equation (30), $\hat{r} = \begin{bmatrix} 0 & -r_z & r_y \\ r_z & 0 & -r_x \\ -r_y & r_x & 0 \end{bmatrix}$ and \hat{r} is a skew matrix which consists of the position vector of joint j_n^p , ($p = 1, 2 \dots 6$), ($n = 1, 2 \dots 6$) in the absolute coordinate frame.

Suppose,

$$A^M = [A_D \quad A_E \quad A_P]^T \quad (36)$$

where $A_D = [(A_D^1)^T \quad (A_D^2)^T \quad \dots \quad (A_D^6)^T]^T$, in which $A_D^1 = \begin{bmatrix} \beta_D^1 \\ a_D^1 \end{bmatrix}$, and A_D^1 is the absolute acceleration of the mass center D at the fixed leg L_{AB}^1 in the absolute coordinate frame.

Suppose,

$$M = \text{diag}[M_D \quad M_E \quad M_P] \quad (37)$$

where $M_D^1 = \begin{bmatrix} J_D^1 & 0 \\ 0 & m_D^1 \mathbf{I} \end{bmatrix}$, and M_D^1 is the mass matrix consisting of J_D^1 , the matrix of mass moment of inertia of the fixed leg L_{AB}^1 , and mass m_D^1 which contains mass of the fixed leg L_{AB}^1 .

Suppose,

$$W^C = [W_D \quad W_E \quad W_P]^T \quad (38)$$

where $W_D = [(W_D^1)^T \quad (W_D^2)^T \quad \dots \quad (W_D^6)^T]^T$, in which $W_D^1 = \begin{bmatrix} \omega_D^1 \times J_D^1 \omega_D^1 \\ m_D^1 \mathbf{g} \end{bmatrix}$, and W_D^1 is a matrix consisting of the inertial torque resulting from Coriolis forces and the force of gravity.

Suppose,

$$W^E = \begin{bmatrix} T_P \\ F_P \end{bmatrix} = \begin{bmatrix} r_P \times F_P \\ F_P \end{bmatrix} = \begin{bmatrix} {}_0D_P(4:6) \times F_P \\ F_P \end{bmatrix} \tag{39}$$

where W^E is the external force vector (if any) acting on the moving platform and is available as a force F_P and a torque T_P in the local coordinate frame of reference, and ${}_0D_P(4:6)$ represents the columns from 4 to 6 of matrix ${}_0D_P$.

Substituting Equations (34)–(39) into Equation (24), the dynamics equation of Gough–Stewart platform can be derived as:

$$CW^S = MA^M + W^C + W^E \tag{40}$$

When the number of constraint wrenches in Gough–Stewart platform is 78, and the sum of Equations (31)–(33) are 78, the wrenches can be calculated by Equation (40),

$$W^S = (CC^T)^{-1} (MA^M + W^C + W^E) \tag{41}$$

5. Numerical Experiment and Discussion

In this section, a prescribed trajectory is used to evaluate the inverse kinematics and dynamics of the Gough–Stewart platform. It has 6 degrees of freedom, including 3 translations and 3 rotations. Suppose that the moving platform follows a spiral trajectory. Here, the parametric equations of the path in displacement, velocity, and acceleration in the absolute coordinate frame are listed in Table A1. With the initial spiral trajectory of the moving platform in Figure 6, the inverse kinematics solutions of the Gough–Stewart platform can be applied directly to the dynamics.

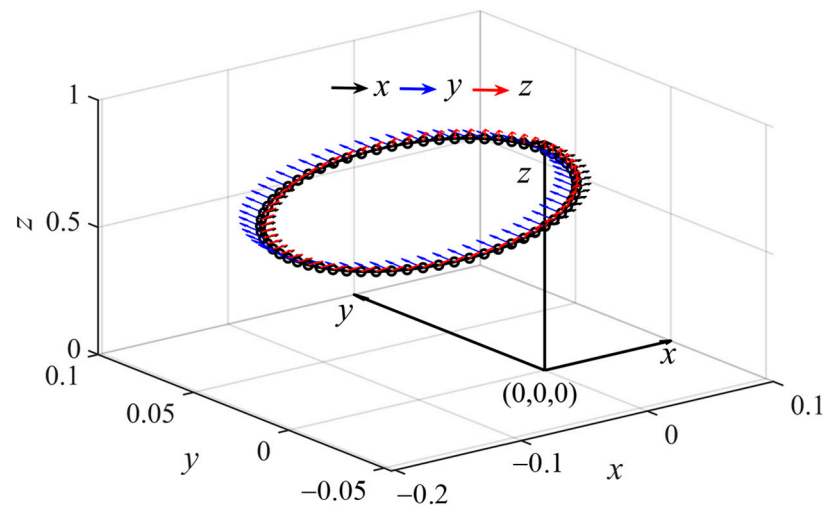


Figure 6. Kinematics analysis of the Gough–Stewart platform.

5.1. Inverse Kinematics Simulation for Gough–Stewart Platform

When the velocity screw of the reference point P on the moving platform is specified in Appendix A Table A1, and the initial conditions of the Gough–Stewart platform are also provided in Tables A2 and A3, the inverse velocity and the inverse displacement (through one-step numerical integration) and acceleration (through one-step numerical differentiation) of the Gough–Stewart platform could be programmed in accordance with the algorithms deduced in Section 3. With the discrete conditions in Table 2 for the numerical calculations, the kinematics parameters can be output by programming in MATLAB. In Figures 7–11, the kinematics of each kinematic chain for the Gough–Stewart platform are all plotted.

Table 2. Discrete conditions for numerical algorithm.

| Initial Condition | Parameters | Value |
|------------------------|------------|--------|
| Total time of the path | $t(s)$ | 10 |
| Interval of iteration | Δt | 0.001 |
| Steps of iteration | k | 10,000 |

Figure 7 illustrates the relative displacements of all joints. Figure 7a shows the angular displacements of all rotational joints, and Figure 7b represents the angular displacement of all prismatic joints. They are all solved by Equation (15) with the one-step numerical algorithm.

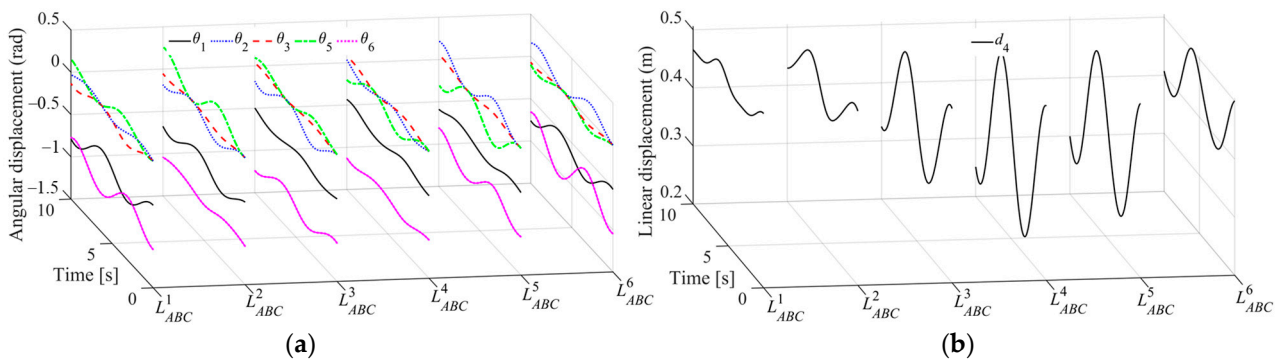


Figure 7. Relative displacements of the joints in each link: (a) relative angular displacements; (b) relative linear displacements.

Figure 8 illustrates the relative velocities of all joints. Figure 8a shows the angular velocities of rotational joints, and Figure 8b shows the angular velocities of prismatic joints. They are all represented by Equation (14) with the one-step numerical algorithm.

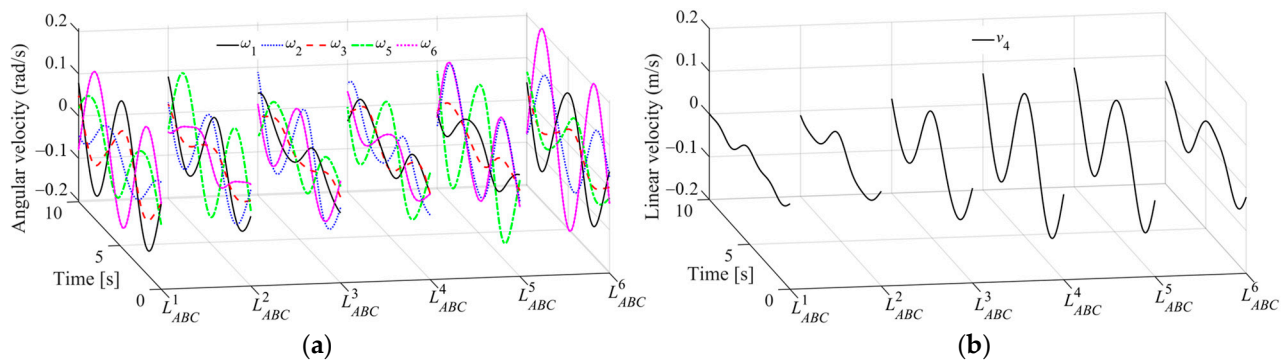


Figure 8. Relative velocities of each joint in each link: (a) relative angular velocities; (b) relative linear velocities.

Figure 9 illustrates the absolute angular velocities of all legs. Figure 9a shows the absolute angular velocities of the fixed legs $L^p_{AB'}$ ($p = 1, 2 \dots 6$), and Figure 9b shows the absolute angular velocities of the moving legs $L^p_{BC'}$ ($p = 1, 2 \dots 6$).

Figure 10 illustrates the absolute accelerations of the fixed legs $L^p_{AB'}$ ($p = 1, 2 \dots 6$) at their individual mass centers. Figure 10a shows the absolute linear accelerations of point D on the fixed legs while Figure 10b illustrates the absolute angular accelerations.

Figure 11 illustrates the absolute accelerations of the moving legs $L^p_{BC'}$ ($p = 1, 2 \dots 6$) at their individual mass centers. Figure 11a shows the absolute linear accelerations of the mass centers of the moving legs, and Figure 11b shows the absolute angular accelerations of the moving legs.

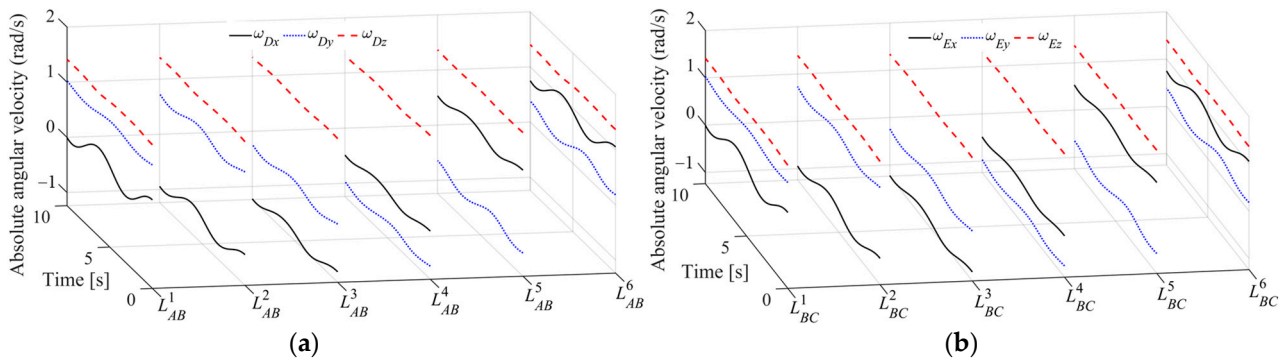


Figure 9. Absolute angular velocities of all legs: (a) absolute angular velocities of the fixed legs L_{AB}^p ($p = 1, 2 \dots 6$); (b) absolute angular velocities of the moving legs L_{BC}^p ($p = 1, 2 \dots 6$).

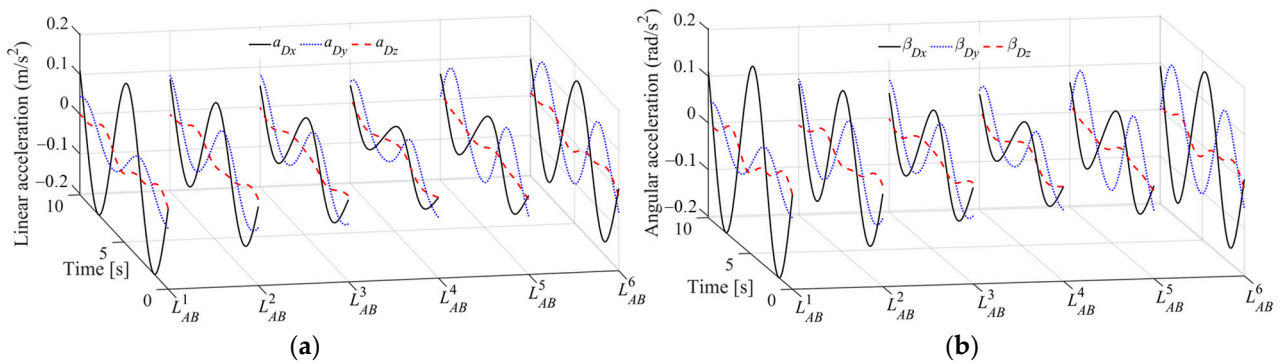


Figure 10. Absolute accelerations of the fixed legs L_{AB}^p ($p = 1, 2 \dots 6$) at their individual mass centers: (a) absolute linear accelerations of the mass centers of the fixed legs; (b) absolute angular accelerations of the fixed legs.

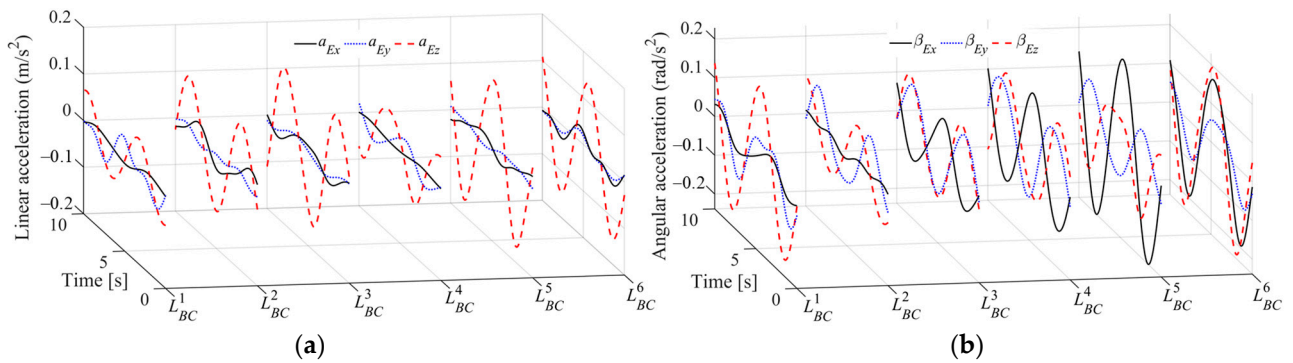


Figure 11. Absolute accelerations of the moving legs L_{BC}^p ($p = 1, 2 \dots 6$) at their respective mass centers: (a) absolute linear accelerations of the mass centers of the moving legs; (b) absolute angular accelerations of the moving legs.

5.2. Inverse Dynamics Simulation for Gough–Stewart Platform

Suppose that the external force exerted on the moving platform at its center point P is $F_P = [0 \ 0 \ 10](N)$, and the torque is $M_P = [10 \ 0 \ 0](Nm)$. With the structure variables, the mass and the mass moment of inertia of each leg of the Gough–Stewart platform listed in Table A4 and the external force and torque applied on the moving platform, the forces and torques of the driving forces F_B^p ($p = 1, 2, \dots, 6$) can be gained (Figure 12) from the dynamics Equation (41). In order to verify this method, we compare the output calculated by vector method and our method. In Figure 12, Method A illustrates the method this paper proposed and Method B presents the method proposed by Dasgupta [11,12].

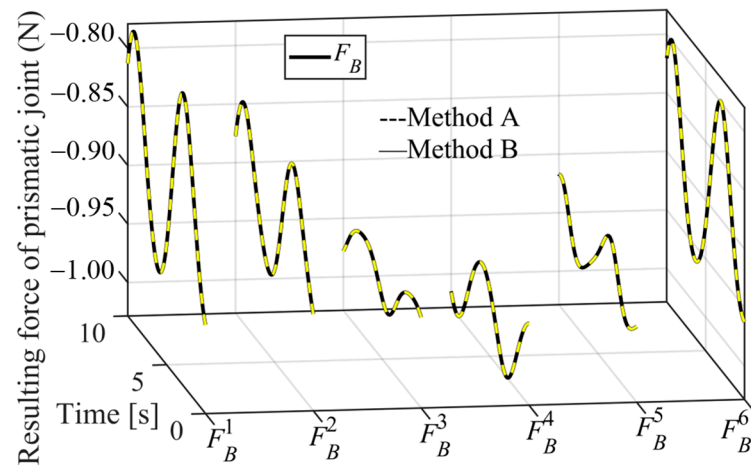


Figure 12. Resultant driving force of each prismatic joint j_B^p , ($p = 1, 2, \dots, 6$).

Figure 12 shows that the resultant driving forces at prismatic joint j_B^p , ($p = 1, 2, \dots, 6$) of the six kinematic chains. In addition, the component forces along the three coordinate frames can be derived from the direction of each chain, and the curves indicate that the driving forces are changing as the moving platform changes.

6. Conclusions

This paper provides a programmable method to solve the kinematics and dynamics of multi-rigid-body systems in screw coordinate. With this method, both displacement and acceleration are uniformly expressed in the matrix form of velocity, and as a result, a one-step numerical algorithm is sufficient to solve them for establishing the dynamics of a multi-rigid-body system. All constraint and driving forces and torques of the multi-rigid-body system can therefore be resolved straightforwardly in the form of screw coordinate. The kinematics and dynamics of the Gough–Stewart platform validate this method which is also suited to analyze a series of multi-rigid-body systems.

Author Contributions: Conceptualization, J.-S.Z., S.-T.W. and X.-C.S.; Methodology, J.-S.Z., S.-T.W. and X.-C.S.; Formal analysis, J.-S.Z., S.-T.W. and X.-C.S.; Writing—original draft, J.-S.Z.; Writing—review & editing, S.-T.W. and X.-C.S. All authors have read and agreed to the published version of the manuscript.

Funding: This work was supported in part by the Basic Research Project Group of China under Grant 514010305-301-3, in part by 2020GQI1003, Guoqiang Research Institute of Tsinghua University, in part by the State Key Laboratory of Tribology, Tsinghua University.

Institutional Review Board Statement: Not applicable.

Informed Consent Statement: Not applicable.

Data Availability Statement: Not applicable.

Conflicts of Interest: The authors declare no conflict of interest.

Nomenclature

| Notation | Description |
|-----------|--|
| ${}_0a_n$ | Linear acceleration of joint j_n with respect to j_0 |
| ${}_0A_n$ | Acceleration of joint j_n with respect to j_0 |
| A^M | Absolute acceleration matrix of a multi-rigid-body system |
| C | Displacement coefficient matrix |
| ${}_0d_n$ | Linear displacement of joint j_n with respect to j_0 |
| ${}_0D_n$ | Displacement of joint j_n with respect to j_0 |
| e_n | Posture vector of joint j_n in the absolute coordinate frame |

- F_n Force vector at joint j_n
- I Identity matrix of 3×3
- 0r_n Position vector of joint j_n in the absolute coordinate frame
- j_n^p The n th joint in the p th kinematic chain
- J_0 Matrix of mass moment of inertia of a single-rigid-body in the absolute coordinate frame
- J_n Matrix of mass moment of inertia of a single-rigid-body at its principal coordinate frame of the mass center
- k Steps of iteration
- l_n^p Length of the n th link in the p th kinematic chain
- L_n^p The n th link in the p th kinematic chain
- m_n Mass of a single-rigid-body
- M Mass matrix
- n Number of joints in a kinematic chain
- p Number of kinematic chains
- R_{0n} Rotation matrix from coordinate frame n to coordinate frame 0.
- S Screw matrix of a multi-rigid-body system
- $\$n$ Unit screw matrix of joint j_n
- t Total time of the path
- Δt Interval of iteration
- T_n Torque vector at joint j_n
- 0V_n Linear velocity of joint j_n with respect to j_0
- ${}^0\dot{V}_n$ Velocity of joint j_n with respect to j_0
- W^S Constraint wrench matrix of the multi-rigid-body system
- W^C Coriolis wrench matrix of the multi-rigid-body system
- W^E External wrench matrix exerted on the multi-rigid-body system
- ${}^0\omega_n$ Angular velocity of joint j_n with respect to j_0
- ${}^0\beta_n$ Angular acceleration of joint j_n with respect to j_0
- ${}^0\theta_n$ Angular displacement of joint j_n with respect to j_0

Appendix A

Table A1. Spiral trajectory of the moving platform.

| Absolute Displacement Vector | Absolute Velocity Vector | Absolute Acceleration Vector |
|---|--|---|
| ${}^0D_E = \begin{bmatrix} 0 \\ 0 \\ 0 \\ 0 \\ 0 \\ \frac{\sqrt{3}}{2} \end{bmatrix} + \begin{bmatrix} -0.1 \cos(t) + 0.1 \\ 0 \\ 0 \\ 0.1 \cos(t) - 0.1 \\ -0.05 \sin(t) \\ 0.1 \cos(t) - 0.1 \end{bmatrix}$ | ${}^0V_E = \begin{bmatrix} 0.1 \sin(t) \\ 0 \\ 0 \\ -0.1 \sin(t) \\ -0.05 \cos(t) \\ -0.1 \sin(t) \end{bmatrix}$ | ${}^0A_E = \begin{bmatrix} 0.1 \cos(t) \\ 0 \\ 0 \\ -0.1 \cos(t) \\ 0.05 \sin(t) \\ -0.1 \cos(t) \end{bmatrix}$ |

Table A2. Initial position of each leg in absolute coordinate frame.

| Leg (m) | Platform (m) | Initial Position of Mass Center |
|--|---|---|
| $\begin{Bmatrix} L_{AB}^p \\ L_{BC}^p \\ L_{AC}^p \end{Bmatrix} = \begin{Bmatrix} 0.05 \\ 0.05 \\ 0.1 \end{Bmatrix}$ | $\begin{Bmatrix} r \\ R \end{Bmatrix} = \begin{Bmatrix} 0.02 \\ 0.05 \end{Bmatrix}$ | $\begin{Bmatrix} r_{d_0}^1 \\ r_{e_0}^1 \\ r_{p_0} \end{Bmatrix} = R_z((p-1)30^\circ) \left\{ \begin{bmatrix} \frac{3}{8} & 0 & \frac{\sqrt{3}}{8} \\ \frac{1}{4} & 0 & \frac{\sqrt{3}}{4} \\ 0 & 0 & 0.1 \end{bmatrix} \right\}, (p = 1, 2 \dots 6)$ |

Table A3. Initial relative displacement of each joint in local coordinate frame.

| | | |
|---|----------------------------------|---|
| ${}^0\theta_1^p(0)(\text{rad})$ | ${}^1\theta_2^p(0)(\text{rad})$ | ${}^2\theta_3^p(0)(\text{rad})$ |
| $\{ {}^0\theta_1^p \} = \{ -\frac{\pi}{6} \}$ | $\{ {}^1\theta_2^p \} = \{ 0 \}$ | $\{ {}^2\theta_3^p \} = \{ 0 \}$ |
| ${}^3d_4^p(0)(\text{m})$ | ${}^4\theta_5^p(0)(\text{rad})$ | ${}^5\theta_6^p(0)(\text{rad})$ |
| $\{ {}^3d_4^p \} = \{ 0.05 \}$ | $\{ {}^4\theta_5^p \} = \{ 0 \}$ | $\{ {}^0\theta_1^p \} = \{ -\frac{\pi}{3} \}$ |

Table A4. Mass and the moments of inertia at mass center and moving platform in local coordinate frame.

| Mass (kg) | Moments of Inertia (kg·m ²) |
|--|--|
| $\begin{cases} m_d^p = 3, (p = 1, 2 \dots 6) \\ m_e^p = 1, (p = 1, 2 \dots 6) \\ m_p = 10 \end{cases}$ | $\begin{cases} \mathbf{J}_{d_0}^p = m_d^p \left[\begin{matrix} (\mathbf{r}_{d_0}^p)^T & \mathbf{r}_{d_0}^p \mathbf{I} - \mathbf{r}_{d_0}^p (\mathbf{r}_{d_0}^p)^T \end{matrix} \right], (p = 1, 2 \dots 6) \\ \mathbf{J}_{e_0}^p = m_e^p \left[\begin{matrix} (\mathbf{r}_{e_0}^p)^T & \mathbf{r}_{e_0}^p \mathbf{I} - \mathbf{r}_{e_0}^p (\mathbf{r}_{e_0}^p)^T \end{matrix} \right], (p = 1, 2 \dots 6) \\ \mathbf{J}_{P_0} = m_p \left[\begin{matrix} (\mathbf{r}_{P_0})^T & \mathbf{r}_{P_0} \mathbf{I} - \mathbf{r}_{P_0} (\mathbf{r}_{P_0})^T \end{matrix} \right] \end{cases}$ |

References

- Gough, V.E.; Whitehall, S.G. Proceedings of the 9th International Congress FISITA, London, UK, 30 April–5 May 1962.
- Fichter, E.F.; Kerr, D.R.; Rees-Jones, J. The Gough-Stewart platform parallel manipulator: A retrospective appreciation. *Proc. Inst. Mech. Eng.* **2009**, *223*, 243–281. [\[CrossRef\]](#)
- Furqan, M.; Suhaib, M.; Ahmad, N. Studies on Stewart platform manipulator: A review. *J. Mech. Sci. Technol.* **2017**, *31*, 4459–4470. [\[CrossRef\]](#)
- Hernández-Vielma, C.; Ortega-Aguilera, R.; Cruchaga, M. Assessment of simultaneous and nested conservative augmented Lagrangian schemes for constrained multibody dynamics. *Proc. Inst. Mech. Eng. Part K J. Multi-Body Dyn.* **2021**, *235*, 271–280. [\[CrossRef\]](#)
- Chen, M.; Zhang, Q.; Qin, X.; Sun, Y. Kinematic, dynamic, and performance analysis of a new 3-DoF over-constrained parallel mechanism without parasitic motion. *Mech. Mach. Theory* **2021**, *162*, 104365. [\[CrossRef\]](#)
- Smith, A.; Yang, C.; Li, C.; Ma, H.; Zhao, L. Development of a dynamics model for the Baxter robot. In Proceedings of the International Conference on Mechatronics and Automation, Harbin, China, 7–10 August 2016; pp. 1244–1249.
- Gallardo-Alvarado, J.; Rodríguez-Castro, R.; Delossantos-Lara, P.J. Kinematics and dynamics of a 4-P RUR Schönflies parallel manipulator by means of screw theory and the principle of virtual work. *Mech. Mach. Theory* **2018**, *122*, 347–360. [\[CrossRef\]](#)
- Azad, F.A.; Yazdi, M.R.H.; Masouleh, M.T. Kinematic and Dynamic Analysis of 3-DOF Delta Parallel Robot Based on the Screw Theory and Principle of Virtual Work. In Proceedings of the 5th Conference on Knowledge Based Engineering and Innovation (KBEI), Tehran, Iran, 28 February–1 March 2019; pp. 717–724.
- Wen, S.; Qin, G.; Zhang, B.; Lam, H.; Zhao, Y.; Wang, H. The study of model predictive control algorithm based on the force/position control scheme of the 5-DoF redundant actuation parallel robot. *Rob. Auton. Syst.* **2016**, *79*, 12–25. [\[CrossRef\]](#)
- Mata, V.; Provenzano, S.; Cuadrado, J.L.; Valero, F. Inverse dynamic problem in robots using Gibbs-Appell equations. *Robotica* **2002**, *20*, 59–67. [\[CrossRef\]](#)
- Dasgupta, B.; Choudhury, P. A Newton-Euler formulation for the inverse dynamics of the Stewart platform manipulator. *Mech. Mach. Theory* **1998**, *33*, 1135–1152. [\[CrossRef\]](#)
- Dasgupta, B.; Mruthyunjaya, T.S. Closed-Form Dynamic Equations of the General Stewart Platform through the Newton-Euler Approach. *Mech. Mach. Theory* **1998**, *33*, 993–1012. [\[CrossRef\]](#)
- Chen, G.; Yu, W.; Li, Q.; Wang, H. Dynamic modeling and performance analysis of the 3-PRRU 1T2R parallel manipulator without parasitic motion. *Nonlinear Dyn.* **2017**, *90*, 339–353. [\[CrossRef\]](#)
- Wang, Z.; Zhao, D.; Zeng, G. The dynamic model of a 6-DOF parallel mechanism. *Mach. Des. Manufact.* **2018**, *S1*, 71–77.
- Niu, A.; Wang, S.; Sun, Y.; Qiu, J.; Qiu, W.; Chen, H. Dynamic modeling and analysis of a novel offshore gangway with 3UPU/UP-RRP series-parallel hybrid structure. *Ocean. Eng.* **2022**, *266*, 113122. [\[CrossRef\]](#)
- Gallardo-Alvarado, J.; Aguilar-Nájera, C.R.; Casique-Rosas, L.; Pérez-González, L.; Rico-Martínez, J.M. Solving the kinematics and dynamics of a modular spatial hyper-redundant manipulator by means of screw coordinate. *Multibody Syst. Dyn.* **2008**, *20*, 307–325. [\[CrossRef\]](#)
- Gallardo-Alvarado, J.; Aguilar-Nájera, C.R.; Casique-Rosas, L.; Rico-Martínez, J.M.; Islam, M.N. Kinematics and dynamics of 2(3-RPS) manipulators by means of screw coordinate and the principle of virtual work. *Mech. Mach. Theory* **2008**, *43*, 1281–1294. [\[CrossRef\]](#)
- Tian, Q.; Xiao, Q.; Sun, Y.; Hu, H.; Liu, H.; Flores, P. Coupling dynamics of a geared multibody system supported by ElastoHydro-Dynamic lubricated cylindrical joints. *Multibody Syst. Dyn.* **2015**, *33*, 259–284. [\[CrossRef\]](#)
- Shan, X.; Gang, C. Nonlinear dynamic behavior of joint effects on a 2(3PUS + S) parallel manipulator. *Proc. Inst. Mech. Eng. Part K J. Multi Body Dyn.* **2018**, *233*, 470–484.
- Asadi, F.; Heydari, A. Analytical dynamic modeling of Delta robot with experimental verification. *Proc. Inst. Mech. Eng. Part K J. Multi-Body Dyn.* **2020**, *234*, 623–630. [\[CrossRef\]](#)
- Liu, C.; Tian, Q.; Hu, H.Y. Dynamics of a large scale rigid-flexible multibody system composed of composite laminated plates. *Multibody Syst. Dyn.* **2011**, *26*, 283–305. [\[CrossRef\]](#)
- Gan, D.; Dai, J.S.; Dias, J.; Seneviratne, L. Forward kinematics solution distribution and analytic singularity-free workspace of linear-actuated symmetrical spherical parallel manipulators. *J. Mech. Robot.* **2015**, *7*, 041007. [\[CrossRef\]](#)
- Dai, J.S.; Jones, J.R. A linear algebraic procedure in obtaining reciprocal screw systems. *J. Robot. Syst.* **2003**, *20*, 401–412. [\[CrossRef\]](#)

24. Hashemi, E.; Khajepour, A. Kinematic and three-dimensional dynamic modeling of a biped robot. *Proc. Inst. Mech. Eng. Part K J. Multi-Body Dyn.* **2017**, *231*, 57–73. [[CrossRef](#)]
25. Shen, H.; Chablat, D.; Zeng, B.; Li, J.; Wu, G.; Yang, T.L. A translational three-degrees-of-freedom parallel mechanism with partial motion decoupling and analytic direct kinematics. *J. Mech. Robot.* **2020**, *12*, 021112. [[CrossRef](#)]
26. Kanaan, D.; Wenger, P.; Chablat, D. Kinematic analysis of a serial-parallel machine tool: The VERNE machine—Science Direct. *Mech. Mach. Theory* **2009**, *44*, 478–498. [[CrossRef](#)]
27. Zhao, J.S.; Wei, S.T.; Ji, J.J. Kinematics of a planar slider-crank linkage in Plücker Coordinate. *Proc. Inst. Mech. Eng. Part C J. Mech. Eng. Sci.* **2022**, *236*, 1588–1597. [[CrossRef](#)]
28. Gallardo-Alvarado, J.; Rico-Martinez, J.M. Kinematics of a hyper-redundant manipulator by means of screw coordinate. *Proc. Inst. Mech. Eng. Part K J. Multi-Body Dyn.* **2009**, *223*, 325–334.

Disclaimer/Publisher’s Note: The statements, opinions and data contained in all publications are solely those of the individual author(s) and contributor(s) and not of MDPI and/or the editor(s). MDPI and/or the editor(s) disclaim responsibility for any injury to people or property resulting from any ideas, methods, instructions or products referred to in the content.